Gate voltage dependent Rashba spin splitting in hole transverse magnetic focusing

M. J. Rendell,[1,*] S. D. Liles,[1,*] A. Srinivasan,[1] O. Klochan,[2,1] I. Farrer,[3,4] D. A. Ritchie,[4] and A. R. Hamilton[1,†]

[1]*School of Physics, University of New South Wales, Sydney, NSW 2052, Australia*
[2]*University of New South Wales Canberra, Canberra, ACT 2600, Australia*
[3]*Department of Electronic and Electrical Engineering, University of Sheffield, Sheffield S1 3JD, United Kingdom*
[4]*Cavendish Laboratory, University of Cambridge, Cambridge CB3 0HE, United Kingdom*

(Received 5 April 2022; accepted 6 June 2022; published 15 June 2022; corrected 6 July 2022)

Magnetic focusing of charge carriers in two-dimensional systems provides a solid state version of a mass spectrometer. In the presence of a spin-orbit interaction, the first focusing peak splits into two spin dependent peaks, allowing focusing to be used to measure spin polarization and the strength of the spin-orbit interaction. In hole systems, the k^3 dependence of the Rashba spin-orbit term allows the spatial separation of spins to be changed *in situ* using a voltage applied to an overall top gate. Here, we demonstrate that this can be used to control the splitting of the magnetic focusing peaks. Additionally, we compare the focusing peak splitting to that predicted by Shubnikov–de Haas oscillations and $k \cdot p$ band-structure calculations. We find that the focusing peak splitting is consistently larger than expected, suggesting further work is needed on understanding spin dependent magnetic focusing.

DOI: 10.1103/PhysRevB.105.245305

I. INTRODUCTION

Magnetic focusing is the solid state realization of a mass spectrometer. Originally proposed as a way to measure the Fermi surface in metals [1,2], it has subsequently been used to probe band structures in graphene [3], spatially separate spin states [4–6], extract electron-electron scattering lengths [7], and measure spin polarization [4,8–11].

In two-dimensional (2D) hole systems in GaAs, magnetic focusing has been used to measure scattering [12,13] and demonstrate the spatial separation of spin [4]. By spatially separating the spin states, the spin polarization in the 2D hole system could be measured using the amplitude of magnetic focusing peaks [4]. This technique was subsequently used to study the transmission of spin by a quantum point contact (QPC) in a focusing setup [10,14].

While previous work on hole magnetic focusing has concentrated on the amplitude of the magnetic focusing peaks, the spacing of the focusing peaks can also be used to obtain information about the spin-orbit interaction of holes. In this paper, we demonstrate control over focusing peak splitting *in situ* using a voltage applied to an overall top gate. We then compare the magnitude of this splitting to predicted values from band-structure calculations and Shubnikov–de Haas oscillations, and find the splitting is consistently larger than expected. This result suggests that focusing peak splitting alone is not a good measure of the Rashba spin-orbit interaction in 2D hole systems.

II. BAND STRUCTURE OF TWO-DIMENSIONAL HOLE SYSTEMS

2D hole systems are fundamentally different from equivalent electron systems. One key difference arises from the form of the Rashba spin-orbit interaction, and this difference can have a dramatic impact on spin-resolved focusing in hole systems.

In hole systems, the Rashba spin-orbit interaction has a k^3 dependence. In GaAs, the subband dispersion for 2D holes with a Rashba spin-orbit interaction (SOI) is given by [15]

$$\mathcal{E}_h = \frac{\hbar^2 k^2}{2m^*} \pm \beta \frac{E_z}{\Delta_{\text{HH-LH}}} k^3, \tag{1}$$

where β is a constant, E_z is the electric field in the out-of-plane direction, and $\Delta_{\text{HH-LH}}$ is the splitting between the heavy-hole (HH) and light-hole (LH) subbands. Figure 1(a) shows the resulting HH subband dispersion for a 2D hole system with Rashba SOI. The Rashba SOI creates two spin dependent k values at the Fermi energy (horizontal dashed line), resulting in a spatial separation of spin in the 2D region. In addition, the magnitude of the Rashba spin-orbit interaction can be changed using a voltage applied to an overall top gate (V_{TG}) on the focusing sample. V_{TG} will change E_z and k, while only having a small effect on $\Delta_{\text{HH-LH}}$. Therefore it is possible to change the magnitude of the Rashba spin-orbit interaction and hence the focusing peak splitting *in situ* by changing V_{TG}. The ability to tune the focusing peak splitting using V_{TG} serves as the focus of this paper.

III. SAMPLE AND MAGNETIC FOCUSING SETUP

Figure 1(b) shows a schematic of a hole transverse magnetic focusing device. A constant current is applied through

*These authors contributed equally to this work.
†alex.hamilton@unsw.edu.au

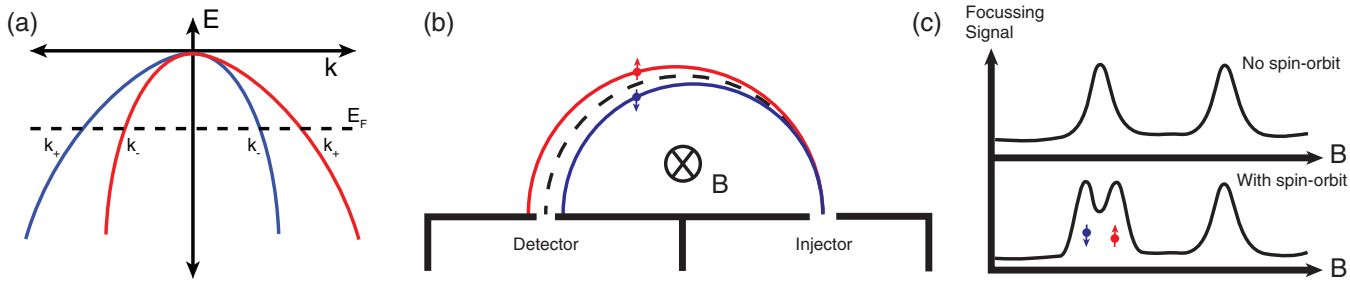

FIG. 1. (a) 2D band dispersion of holes with a Rashba SOI. The k^3 Rashba term splits the first heavy-hole subband into two spin chiralities (red and blue curves). This results in two spin dependent values of momentum (k_+ and k_-) at the Fermi energy (dashed horizontal line). (b) Schematic of magnetic focusing with a spin-orbit interaction. The black dashed line represents the classical focusing trajectory in the absence of a spin-orbit interaction. When a spin-orbit interaction is present, two spin dependent trajectories are created (blue and red paths). (c) Focusing peaks with and without a spin-orbit interaction. In the presence of a spin-orbit interaction the first focusing peak splits into two spin-dependent peaks.

the injector and a perpendicular out-of-plane magnetic field causes holes to form cyclotron orbits. The detector voltage is measured as a function of magnetic field strength, and peaks in the focusing signal occur when the focusing diameter matches the distance between injector and detector. In the absence of a spin-orbit interaction, the holes follow a single trajectory (black dashed line). In the presence of a spin-orbit interaction, the focusing trajectory becomes spin dependent (red and blue lines) [4,16,17]. Figure 1(c) compares the focusing signal with and without a spin-orbit interaction. When there is a spin-orbit interaction, the first focusing peak splits into two spin dependent peaks. This splitting of the first peak has been used to measure the strength of the spin-orbit interaction [4]. The second focusing peak does not split due to boundary reflection causing a refocusing of the spin dependent trajectories [18,19].

To investigate the V_{TG} dependence of hole focusing, a magnetic focusing sample was fabricated on an undoped, accumulation mode GaAs/$Al_{0.33}Ga_{0.67}As$ heterostructure. The heterostructure is shown in Fig. 2(a), and consists of a 15-nm GaAs quantum well (QW) 85 nm below the wafer surface [Fig. 2(b)]. In order to accumulate a 2D hole gas (2DHG) in the well, 30 nm of Al_2O_3 is deposited using atomic layer deposition to act as a gate oxide, followed by an overall Ti/Au top gate. The high quality of the heterostructure ensures that the hole mobility ($\mu = 5.4$–$7.6\times10\ \mathrm{cm}^{-2}/\mathrm{V\ s}$) and mean free path ($l_{mfp} = 2.4$–$5.3\ \mu$m) is sufficient to perform magnetic focusing.

The asymmetric potential confining the 2D holes leads to a Rashba splitting of the valence band [Fig. 2(c)] creating a difference in momentum between the spin chiralities which is detected using magnetic focusing [4]. We use NEXTNANO [20] to calculate the subband energies and $E(k)$ dispersions of the two-dimensional hole system (2DHS). The NEXTNANO calculations employ a combination of a Schrödinger-Poisson solver and a $6\times6\ k\cdot p$ calculation for our sample heterostructure. The calculations include the Rashba SOI term but do not include contributions from the Dresselhaus SOI. Figure 2(c) shows the calculated HH1 subband dispersion for our sample, with a different k_F visible at the Fermi energy (dashed horizontal line) for the two different spin states. The different k_F results in a different cyclotron radius for each spin (HH+ and HH−), causing a spatial separation of spin in the 2D region in focusing [4].

A scanning electron microscope (SEM) image of the device before the top gate is deposited is shown in Fig. 2(d).

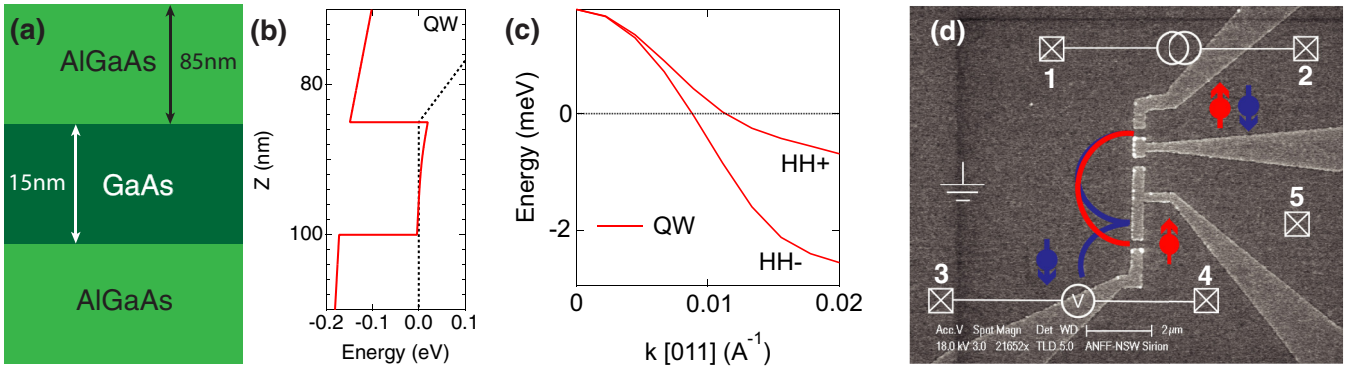

FIG. 2. (a) Schematic of the QW wafer: a 15-nm GaAs quantum well in a GaAs/$Al_{0.33}Ga_{0.67}As$ heterostructure (wafer W713). (b) The square well confining potential created by the heterostructure in (a) from a Schrödinger-Poisson calculation using NEXTNANO. (c) Band dispersion of the spin-split HH subbands for the QW, calculated using a $6\times6\ k\cdot p$ solver (NEXTNANO). (d) SEM image of the magnetic focusing lithography with an overlaid electrical setup. Red and blue semicircles show the trajectories of different spins in the presence of a spin-orbit interaction. Three different focusing diameters (d_{Focus}) are available through use of different QPC combinations: 800, 2300, and 3100 nm.

Metal split gates are used to define 1D quantum point contacts (QPCs) used to inject and detect the focused beam. The QPCs are symmetrically biased (minimal ΔV_{SG}) to the $G = 2e^2/h$ conductance plateau to allow for the injection and detection of both spin chiralities [10]. Symmetrically biasing the QPCs at $G = 2e^2/h$ also avoids the complex structure of the first hole subband [21] and additional spin dynamics created by the QPC [6]. A constant current (5 nA) is injected through one QPC (contacts 1 and 2) using a lock-in amplifier, while the voltage buildup is measured across a second QPC (contacts 3 and 4), allowing a four-terminal focusing resistance to be measured ($R_{Focus} = V_{34}/I_{12}$). A perpendicular out-of-plane magnetic field is applied (B_{Focus}) which causes the holes to follow spin dependent cyclotron orbits, indicated by the red and blue lines in Fig. 2(d). When the diameter of a cyclotron orbit matches the distance between the injector and collector QPC, charge builds up in the collector and a peak in the collector voltage (and hence R_{Focus}) is observed. In the absence of a spin-orbit interaction the magnetic focusing peaks occur at magnetic fields given by [22]

$$B_{Focus} = \frac{2\hbar k_F}{e d_{Focus}}, \tag{2}$$

where k_F is the Fermi momentum and d_{Focus} is the distance between injector and collector QPC (focusing diameter). In the presence of a Rashba SOI, the first focusing peak splits due to the spin-dependent cyclotron orbits in the 2D region [4,16,19].

The choice of d_{Focus} is an important trade-off in magnetic focusing. Increasing d_{Focus} has the benefit of increasing the resolution of the focusing peaks, as the width of the QPC becomes a smaller fraction of the focusing diameter [13,22]. A larger d_{Focus} also causes the focusing peaks to occur at lower B_{Focus}, which will reduce the impact of Zeeman splitting and Shubnikov–de Haas oscillations on the focusing peaks. However, if d_{Focus} is made too large the focusing path length will approach the mean free path and scattering will cause significant attenuation of the focusing peaks.

IV. TOP GATE DEPENDENCE OF FOCUSING PEAK SPLITTING

In this section we use the voltage applied to the overall top gate of our sample to change the strength of the Rashba SOI and hence focusing peak splitting. As discussed in Sec. II, the Rashba spin-orbit term in 2D hole systems is given by

$$\mathcal{H}_R \propto \beta \frac{E_z}{\Delta_{HH\text{-}LH}} k^3, \tag{3}$$

where E_z is the electric field across the 2D interface, $\Delta_{HH\text{-}LH}$ is the splitting between the heavy-hole (HH) and light-hole (LH) levels in the quantum well, and k is the Fermi momentum. Increasing $|V_{TG}|$ increases both E_z and k_F, while only causing a slight increase in $\Delta_{HH\text{-}LH}$ due to the quantum well confinement. The net result is an increase in the magnitude of $\mathcal{H}_R$ as $|V_{TG}|$ is increased, which causes an increase in the splitting of the first focusing peak.

Figure 3(a) shows focusing measurements for four different values of V_{TG}. V_{TG} was first set to -1.15 V, corresponding to a density of $n_{2D} = 0.83\times10^{11}$ cm^{-2} (bottom trace, yellow).

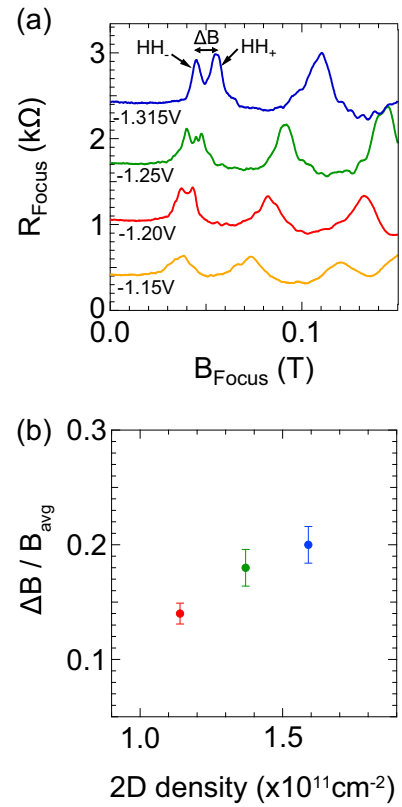

FIG. 3. (a) Focusing for different V_{TG}. $d_{Focus} = 2300$ nm. More negative V_{TG} results in a larger n_{2D} and stronger Rashba SOI, increasing the splitting of the first focusing peak. (b) Splitting between the magnetic focusing peaks as a function of n_{2D}. n_{2D} was found from the Hall slope at the same V_{TG} as the focusing data. Error bars are the uncertainty in the peak position of a double Gaussian fit.

Multiple evenly spaced focusing peaks can be observed, indicating low scattering and specular reflections from the gates [22]. Additionally, the location of all focusing peaks is consistent with the location predicted by Eq. (2). At $V_{TG} = -1.15$ V the Rashba SOI is not yet large enough to resolve a spin-split first focusing peak. As V_{TG} is made more negative, n_{2D} increases and we observe multiple effects on the focusing peaks. First, the focusing peaks move to higher B_{Focus} since k_F increases [Eq. (2)]. Second, there is an increase in the amplitude of the focusing peaks. This is due to an increase of the hole velocity, which causes a reduction in scattering as the holes travel through the 2D region from injector to detector.

The third effect of increasing V_{TG} is to increase the Rashba splitting of the HH states, causing the first focusing peak to split. At $V_{TG} = -1.20$ V (red trace) the first focusing peak develops into a double peak, as the spin splitting is now able to be resolved. At $V_{TG} = -1.25$ V (green trace) the splitting of the first focusing peak is larger (with some additional structure due to branching flow and interference effects) [19,22–24]. At the most negative $V_{TG} = -1.315$ V (top trace, blue) the spin-split first peak can be completely resolved. This increase in splitting is qualitatively as expected, as a more negative V_{TG} increases the Rashba SOI.

We now quantify the splitting of the first focusing peak. To measure the peak splitting, a double Gaussian is fit to the

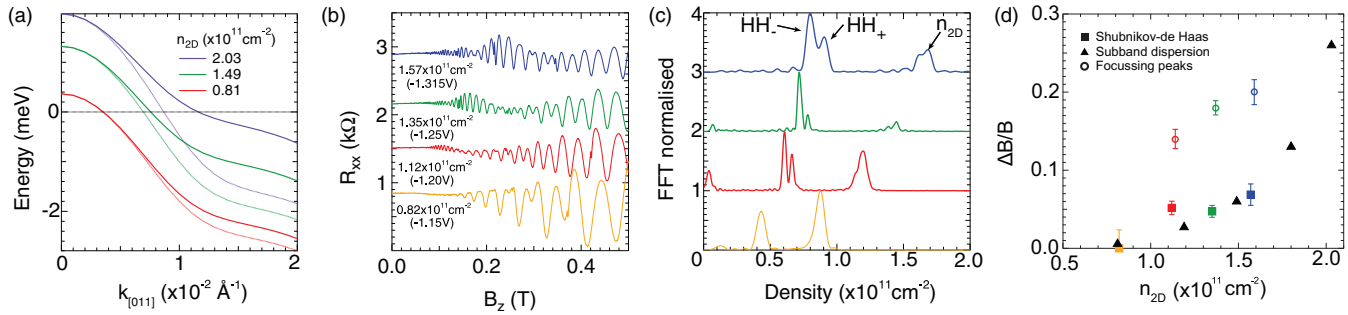

FIG. 4. Comparing focusing peak splitting to NEXTNANO subband dispersion and Shubnikov–de Haas oscillations. (a) Dispersion of the HH subbands at different n_{2D} from a 6×6 $k \cdot p$ NEXTNANO calculation. Solid lines indicate the HH+ subband, while dashed lines indicate HH−. (b) Shubnikov–de Haas oscillations obtained from the focusing sample. (c) FFT of the oscillations in (a). Peaks correspond to the density of each spin chirality (HH+ and HH−) and the total density (n_{2D}). (d) Comparison of the predicted focusing peak splitting from Shubnikov–de Haas (solid squares) and NEXTNANO (solid triangles) to the measured focusing peak splitting (open circles).

first focusing peak doublet to find the peak spacing (ΔB). Since the magnitude of ΔB will depend on d_{Focus} [see Eq. (2)], the dependence on d_{Focus} can be removed by dividing by the central peak location (B_{avg}). Figure 3(b) shows the normalized splitting ($\Delta B/B_{\text{avg}}$) as a function of n_{2D}. An increase in the peak splitting is seen as V_{TG} is made more negative (larger n_{2D}), with $\Delta B/B_{\text{avg}}$ approaching 0.2 (i.e., the splitting is approximately 20% of $\hbar\omega_c$). The lowest density is not included in Fig. 3(b) as a splitting of the first peak cannot be resolved.

These results show that it is possible to tune the spatial separation of spins in a 2D hole system using only a voltage applied to a top gate. In addition, the separation can be tuned over a wide range within the same sample—from too small to resolve (at $V_{\text{TG}} = -1.15$ V) to complete separation (at $V_{\text{TG}} = -1.315$ V). This tunable spin separation makes 2D hole systems ideal for studying the spatial separation of spin states.

V. COMPARING FOCUSING TO BAND-STRUCTURE CALCULATIONS AND SHUBNIKOV–DE HAAS OSCILLATIONS

Next, we compare the splitting of the first magnetic focusing peak to a predicted splitting from other methods. We use two methods to predict the focusing peak splitting: band-structure calculations (using NEXTNANO) and Shubnikov–de Haas measurements.

Figure 4(a) shows the calculated HH subband from NEXTNANO over the density range of our sample. As n_{2D} is increased (more negative V_{TG}) the HH subband splits into two spin chiralities (HH+ and HH−). From the values of k_+ and k_- at the Fermi energy ($E_F = 0$) it is possible to predict a focusing peak splitting ($\Delta B/B_{\text{avg}}$). Equation (2) shows that $\Delta k/k_F = \Delta B/B_{\text{avg}}$ where $\Delta k = k_{\text{HH+}} - k_{\text{HH−}}$. (This approximation is valid provided $\Delta k/k_F \ll 1$.)

Shubnikov–de Haas oscillations can also be used to predict a focusing peak splitting. In the absence of a spin-orbit interaction, Shubnikov–de Haas oscillations are periodic in $1/B$, with a frequency proportional to n ($f = nh/e$). The addition of a spin-orbit interaction creates two Fermi surfaces, each with a different spin chirality. The Fermi surfaces have different areas, resulting in two distinct frequencies in Shubnikov–de Haas oscillations [25,26] which can be used to predict the splitting of magnetic focusing peaks.

Figure 4(b) shows Shubnikov–de Haas oscillations measured at the same V_{TG} (same n_{2D}) as the focusing measurement on the same sample. To predict a focusing peak splitting ($\Delta B/B_{\text{avg}}$) the density of each spin chirality is found from a fast Fourier transform (FFT) of the Shubnikov–de Haas oscillations [Fig. 4(c)]. These densities are then used to find the momentum of each chirality ($k = \sqrt{4\pi n}$). ΔB can then be found by substituting k into Eq. (2). Similarly, B_{avg} can be found by substituting $k_F = \sqrt{2\pi n_{2D}}$ into Eq. (2).

Finally, we compare the measured focusing peak splitting to a predicted splitting from $k \cdot p$ calculations and Shubnikov–de Haas oscillations in Fig. 4(d). There is good agreement between Shubnikov–de Haas measurements (colored squares) and NEXTNANO calculations (black triangles). However, the splitting of the magnetic focusing peaks (open circles) is consistently larger than the value predicted by NEXTNANO or Shubnikov–de Haas measurements. This suggests that the focusing peak splitting does not only depend the magnitude of the Rashba SOI.

To ensure that the split gates on the focusing sample did not affect the 2D measurement, Shubnikov–de Haas oscillations were also measured on a Hall bar fabricated on the same wafer as the focusing sample (W713). An FFT was also performed on the Hall bar data, and this was used to predict a focusing peak splitting. The predicted peak splitting from the Hall bar was in good agreement with the predicted peak splitting from the focusing sample [within the uncertainty shown in Fig. 4(c)]. This result demonstrates that the gates used to define the focusing geometry do not affect the Shubnikov–de Haas measurements on the focusing sample.

Some additional explanations for the larger than expected splitting of the magnetic focusing peaks can also be ruled out. Comparing the focusing peak splitting with a 2D measurement (Shubnikov–de Haas oscillations) rules out any 2D effects such as Fermi-surface distortion as this should also affect Shubnikov–de Haas measurements. Effects from lateral biasing of the QPC split gates [6] can also be ruled out, as all measurements were performed with the split gates biased as symmetrically as possible to remain on the $G = 2e^2/h$

conductance plateau. Problems with the magnet used to create B_{Focus} are also unlikely. The hysteresis of the magnet has been fully corrected and the magnitude of the magnetic field was verified using a Hall sensor on the sample probe. One possibility is additional complex spin dynamics created by the injector and detector QPCs. These dynamics could be created by the rapid spatial variation of the electrostatic potential in the injector and collector QPC, which may lead to nonadiabatic spin evolution [27]. Additionally, recent theoretical work has found coupling between gate electric fields and heavy-hole/light-hole bands in GaAs [28]. This coupling may also be significant in the presence of a magnetic field, as in a focusing measurement, and could account for the larger focusing peak spacing. However, for this to be the cause it would need to affect only the focusing and not other 2D measurements such as Shubnikov–de Haas oscillations.

The most likely explanation for the difference between the predicted and measured focusing peak spacing is linear-in-k SOI terms [29–31]. These terms should not affect the Shubnikov–de Haas oscillations as these require the hole spins to form a closed loop. This is in contrast to a focusing setup where the holes only travel a semicircular path, and hence could be sensitive to k-linear SOI terms. In addition, these k-linear terms were not included in NEXTNANO calculations, which would explain the agreement between the calculations and Shubnikov–de Haas measurements. As the k-linear SOI terms have a crystal orientation dependence, additional measurements with focusing samples in different crystal orientations may be able to confirm the influence of k-linear SOI terms on hole magnetic focusing.

VI. CONCLUSIONS

In this paper we have investigated the gate voltage dependence of magnetic focusing in hole systems with a Rashba spin-orbit interaction. We demonstrated control over the focusing peak splitting using the voltage applied to an overall top gate, showing that the splitting can be tuned from too small to resolve to a complete separation of the spin peaks. The magnitude of the peak splitting was compared to Shubnikov–de Haas oscillations and band-structure calculations, and we found that the peak splitting is consistently larger than expected. This result may indicate the presence of complex spin dynamics or influences from k-linear SOI terms which can only be detected in focusing measurements [27–31]. While further work is required to determine the exact cause of the larger than expected peak spacing, this result suggests that care must be take when quantitatively relating the spacing of hole focusing peaks to the size of the Rashba spin-orbit interaction.

ACKNOWLEDGMENTS

The authors would like to thank S. Bladwell, O. P. Sushkov, D. Culcer, E. Y. Sherman, and U. Zülicke for valuable discussions. Devices were fabricated at the UNSW node of the Australian National Fabrication Facility (ANFF). This research was funded by the Australian Government through the Australian Research Council Discovery Project Scheme and CoE Scheme (Grant No. CE170100039), and by the UK Engineering and Physical Sciences Research Council (Grant No. EP/R029075/1).

[1] Y. Sharvin, A possible method for studying Fermi surfaces, Sov. Phys. JETP **48**, 984 (1965).
[2] V. Tsoi, Focusing of electrons in a metal by a transverse magnetic field, Sov. Phys. JETP **19**, 114 (1974).
[3] T. Taychatanapat, K. Watanabe, T. Taniguchi, and P. Jarillo-Herrero, Electrically tunable transverse magnetic focusing in graphene, Nat. Phys. **9**, 225 (2013).
[4] L. P. Rokhinson, V. Larkina, Y. B. Lyanda-Geller, L. N. Pfeiffer, and K. W. West, Spin Separation in Cyclotron Motion, Phys. Rev. Lett. **93**, 146601 (2004).
[5] J. J. Heremans, H. Chen, M. B. Santos, N. Goel, W. Van Roy, and G. Borghs, Spin-dependent transverse magnetic focusing in InSb- and InAs-based heterostructures, AIP Conf. Proc. **893**, 1287 (2007).
[6] S.-T. Lo, C.-H. Chen, J.-C. Fan, L. W. Smith, G. L. Creeth, C.-W. Chang, M. Pepper, J. P. Griffiths, I. Farrer, H. E. Beere, G. A. C. Jones, D. A. Ritchie, and T.-M. Chen, Controlled spatial separation of spins and coherent dynamics in spin-orbit-coupled nanostructures, Nat. Commun. **8**, 15997 (2017).
[7] A. Gupta, J. J. Heremans, G. Kataria, M. Chandra, S. Fallahi, G. C. Gardner, and M. J. Manfra, Precision measurement of electron-electron scattering in GaAs/AlGaAs using transverse magnetic focusing, Nat. Commun. **12**, 5048 (2021).
[8] R. M. Potok, J. A. Folk, C. M. Marcus, and V. Umansky, Detecting Spin-Polarized Currents in Ballistic Nanostructures, Phys. Rev. Lett. **89**, 266602 (2002).
[9] J. A. Folk, R. M. Potok, C. M. Marcus, and V. Umansky, A gate-controlled bidirectional spin filter using quantum coherence, Science **299**, 679 (2003).
[10] L. P. Rokhinson, L. N. Pfeiffer, and K. W. West, Spontaneous Spin Polarization in Quantum Point Contacts, Phys. Rev. Lett. **96**, 156602 (2006).
[11] T. M. Chen, M. Pepper, I. Farrer, G. A. C. Jones, and D. A. Ritchie, All-Electrical Injection and Detection of a Spin-Polarized Current Using 1D Conductors, Phys. Rev. Lett. **109**, 177202 (2012).
[12] J. Heremans, M. Santos, and M. Shayegan, Observation of magnetic focusing in two-dimensional hole systems, Appl. Phys. Lett. **61**, 1652 (1992).
[13] M. Rendell, O. Klochan, A. Srinivasan, I. Farrer, D. Ritchie, and A. Hamilton, Transverse magnetic focussing of heavy holes in a (100) GaAs quantum well, Semicond. Sci. Technol. **30**, 102001 (2015).
[14] S. Chesi, G. F. Giuliani, L. P. Rokhinson, L. N. Pfeiffer, and K. W. West, Anomalous Spin-Resolved Point-Contact Transmission of Holes due to Cubic Rashba Spin-Orbit Coupling, Phys. Rev. Lett. **106**, 236601 (2011).
[15] R. Winkler, *Spin-Orbit Coupling Effects in Two-Dimensional Electron and Hole Systems* (Springer, Berlin, 2003).
[16] U. Zülicke, J. Bolte, and R. Winkler, Magnetic focusing of charge carriers from spin-split bands: Semiclassics of a Zitter-Bewegung effect, New J. Phys. **9**, 355 (2007).

[17] S. Bladwell and O. P. Sushkov, Magnetic focusing of electrons and holes in the presence of spin-orbit interactions, Phys. Rev. B **92**, 235416 (2015).

[18] G. Usaj and C. A. Balseiro, Transverse electron focusing in systems with spin-orbit coupling, Phys. Rev. B **70**, 041301(R) (2004).

[19] Y. K. Lee, J. S. Smith, and J. H. Cole, Influence of device geometry and imperfections on the interpretation of transverse magnetic focusing experiments, Nanoscale Res. Lett. **17**, 31 (2022).

[20] http://www.nextnano.de/.

[21] K. L. Hudson, A. Srinivasan, O. Goulko, J. Adam, Q. Wang, L. A. Yeoh, O. Klochan, I. Farrer, D. A. Ritchie, A. Ludwig, A. D. Wieck, J. von Delft, and A. R. Hamilton, New signatures of the spin gap in quantum point contacts, Nat. Commun. **12**, 5 (2021).

[22] H. van Houten, C. W. J. Beenakker, J. G. Williamson, M. E. I. Broekaart, P. H. M. van Loosdrecht, B. J. van Wees, J. E. Mooij, C. T. Foxon, and J. J. Harris, Coherent electron focusing with quantum point contacts in a two-dimensional electron gas, Phys. Rev. B **39**, 8556 (1989).

[23] K. Aidala, R. Parrott, T. Kramer, E. Heller, R. Westervelt, M. Hanson, and A. Gossard, Imaging magnetic focusing of coherent electron waves, Nat. Phys. **3**, 464 (2007).

[24] S. Bladwell and O. P. Sushkov, Interference effects and Huygens principle in transverse magnetic focusing of electrons and holes, Phys. Rev. B **96**, 035413 (2017).

[25] H. L. Stormer, Z. Schlesinger, A. Chang, D. C. Tsui, A. C. Gossard, and W. Wiegmann, Energy Structure and Quantized Hall Effect of Two-Dimensional Holes, Phys. Rev. Lett. **51**, 126 (1983).

[26] S. J. Papadakis, E. P. De Poortere, H. C. Manoharan, M. Shayegan, and R. Winkler, The effect of spin splitting on the metallic behavior of a two-dimensional system, Science **283**, 2056 (1999).

[27] D. Culcer, C. Lechner, and R. Winkler, Spin Precession and Alternating Spin Polarization in Spin-3/2 Hole Systems, Phys. Rev. Lett. **97**, 106601 (2006).

[28] P. Philippopoulos, S. Chesi, D. Culcer, and W. A. Coish, Pseudospin-electric coupling for holes beyond the envelope-function approximation, Phys. Rev. B **102**, 075310 (2020).

[29] E. Rashba and E. Sherman, Spin-orbital band splitting in symmetric quantum wells, Phys. Lett. A **129**, 175 (1988).

[30] J.-W. Luo, A. N. Chantis, M. van Schilfgaarde, G. Bester, and A. Zunger, Discovery of a Novel Linear-in-k Spin Splitting for Holes in the 2D GaAs/AlAs System, Phys. Rev. Lett. **104**, 066405 (2010).

[31] M. V. Durnev, M. M. Glazov, and E. L. Ivchenko, Spin-orbit splitting of valence subbands in semiconductor nanostructures, Phys. Rev. B **89**, 075430 (2014).

Correction: A name and grant number were missing in the Acknowledgments and have been fixed.